

## **RGS4 Regulates Parasympathetic Signaling and Heart Rate Control in the Sinoatrial Node**

Carlo Cifelli, Robert A. Rose, Hangjun Zhang, Julia Voigtlaender-Bolz, Steffen-Sebastian Bolz, Peter H. Backx and Scott P. Heximer

*Circ. Res.* 2008;103;527-535; originally published online Jul 24, 2008;

DOI: 10.1161/CIRCRESAHA.108.180984

Circulation Research is published by the American Heart Association, 7272 Greenville Avenue, Dallas, TX 75214

Copyright © 2008 American Heart Association. All rights reserved. Print ISSN: 0009-7330. Online ISSN: 1524-4571

The online version of this article, along with updated information and services, is located on the World Wide Web at:

<http://circres.ahajournals.org/cgi/content/full/103/5/527>

Data Supplement (unedited) at:

<http://circres.ahajournals.org/cgi/content/full/CIRCRESAHA.108.180984/DC1>

Subscriptions: Information about subscribing to Circulation Research is online at  
<http://circres.ahajournals.org/subscriptions/>

Permissions: Permissions & Rights Desk, Lippincott Williams & Wilkins, a division of Wolters Kluwer Health, 351 West Camden Street, Baltimore, MD 21202-2436. Phone: 410-528-4050. Fax: 410-528-8550. E-mail:  
[journalpermissions@lww.com](mailto:journalpermissions@lww.com)

Reprints: Information about reprints can be found online at  
<http://www.lww.com/reprints>

# RGS4 Regulates Parasympathetic Signaling and Heart Rate Control in the Sinoatrial Node

Carlo Cifelli,\* Robert A. Rose,\* Hangjun Zhang, Julia Voigtlaender-Bolz, Steffen-Sebastian Bolz, Peter H. Backx, Scott P. Heximer

**Abstract**—Heart rate is controlled by the opposing activities of sympathetic and parasympathetic inputs to pacemaker myocytes in the sinoatrial node (SAN). Parasympathetic activity on nodal myocytes is mediated by acetylcholine-dependent stimulation of  $M_2$  muscarinic receptors and activation of  $G\alpha_{i/o}$  signaling. Although regulators of G protein signaling (RGS) proteins are potent inhibitors of  $G\alpha_{i/o}$  signaling in many tissues, the RGS protein(s) that regulate parasympathetic tone in the SAN are unknown. Our results demonstrate that RGS4 mRNA levels are higher in the SAN compared to right atrium. Conscious freely moving RGS4-null mice showed increased bradycardic responses to parasympathetic agonists compared to wild-type animals. Moreover, anesthetized RGS4-null mice had lower baseline heart rates and greater heart rate increases following atropine administration. Retrograde-perfused hearts from RGS4-null mice showed enhanced negative chronotropic responses to carbachol, whereas SAN myocytes showed greater sensitivity to carbachol-mediated reduction in the action potential firing rate. Finally, RGS4-null SAN cells showed decreased levels of G protein-coupled inward rectifying potassium (GIRK) channel desensitization and altered modulation of acetylcholine-sensitive potassium current ( $I_{KACH}$ ) kinetics following carbachol stimulation. Taken together, our studies establish that RGS4 plays an important role in regulating sinus rhythm by inhibiting parasympathetic signaling and  $I_{KACH}$  activity. (*Circ Res.* 2008;103:527-535.)

**Key Words:** RGS proteins ■ sinoatrial node ■ parasympathetic ■ GIRK channels

Heart rate (HR) regulation by the autonomic nervous system is integrated by specialized autorhythmic (pacemaker) cells located within the sinoatrial node (SAN). Sympathetic neurotransmitters work via  $G_s$ -coupled  $\beta$ -adrenergic receptors to increase adenylyl cyclase activity, intracellular cAMP concentration and protein kinase A activity. As a result, cAMP-regulated effectors such as hyperpolarization-activated cyclic nucleotide-gated cation (HCN) channels, delayed rectifier, and voltage-gated  $Ca^{2+}$  channels are enlisted by sympathetic activity to increase pacemaker cell firing rate.<sup>1,2</sup> By contrast, vagal parasympathetic activity decreases HR via  $G\alpha_{i/o}$ -coupled cholinergic  $M_2$  muscarinic receptors ( $M_2R$ s). Several effects, mediated by both  $G\alpha_{i/o}$  and  $G\beta\gamma$  subunits, may contribute to this reduction in HR.  $G\beta\gamma$  heterodimers directly activate G protein-coupled inward rectifying potassium (GIRK) channels, resulting in membrane hyperpolarization. By contrast,  $G\alpha_{i/o}$  can both modulate phosphodiesterase activity and inhibit adenylyl cyclase activity, leading to decreased depolarizing currents carried by HCN and L-type calcium channels.<sup>2-5</sup> Because dysregu-

lation of parasympathetic activity occurs in heart failure, sick sinus syndrome, and selected cardiac arrhythmias,<sup>6</sup> it is of clinical interest to identify key molecular regulators of parasympathetic signaling.

Regulators of G protein signaling (RGS) function as GTPase-activating proteins (GAPs) for  $G\alpha$  subunits via a conserved  $\approx 110$  kDa RGS box domain.<sup>7,8</sup> Accordingly, RGS proteins induce faster termination of signaling following removal of G protein-coupled receptor (GPCR) agonists. These proteins have recently emerged as inhibitory candidates of parasympathetic signaling in autorhythmic cells of the SAN because expression of RGS-resistant  $G\alpha_{i2}$  or  $G\alpha_o$  in mice reduced pacemaker cell automaticity.<sup>9,10</sup> However, the pan-specific RGS protein inhibition in these models precluded identification of the specific RGS proteins involved. Although a large number of mammalian RGS proteins are expressed in the heart,<sup>11-13</sup> their specific roles as regulators of parasympathetic pathway effectors are not well understood. Because RGS4 interacts with both  $M_2R$ <sup>14</sup> and GIRK channels,<sup>15</sup> and because it can also modulate GIRK channel activation,<sup>16,17</sup> we investigated its role as a regulator of

Original received February 12, 2008; resubmission received June 9, 2008; revised resubmission received July 9, 2008; accepted July 10, 2008.

From the Department of Physiology (C.C., R.A.R., H.Z., J.V.-B., S.-S.B., P.H.B., S.P.H.), Heart and Stroke/Richard Lewar Centre of Excellence in Cardiovascular Research, University of Toronto; and Department of Medicine (R.A.R., P.H.B.), University of Toronto, and Division of Cardiology, University Health Network, Toronto, Ontario, Canada.

\*Both authors contributed equally to this work.

Correspondence to Scott P. Heximer, Canada Research Chair in Cardiovascular Physiology, Heart and Stroke/Richard Lewar Centre of Excellence in Cardiovascular Research, University of Toronto, 1 King's College Circle, Toronto, Ontario M5S 1A8, Canada. E-mail scott.heximer@utoronto.ca

© 2008 American Heart Association, Inc.

*Circulation Research* is available at <http://circres.ahajournals.org>

DOI: 10.1161/CIRCRESAHA.108.180984

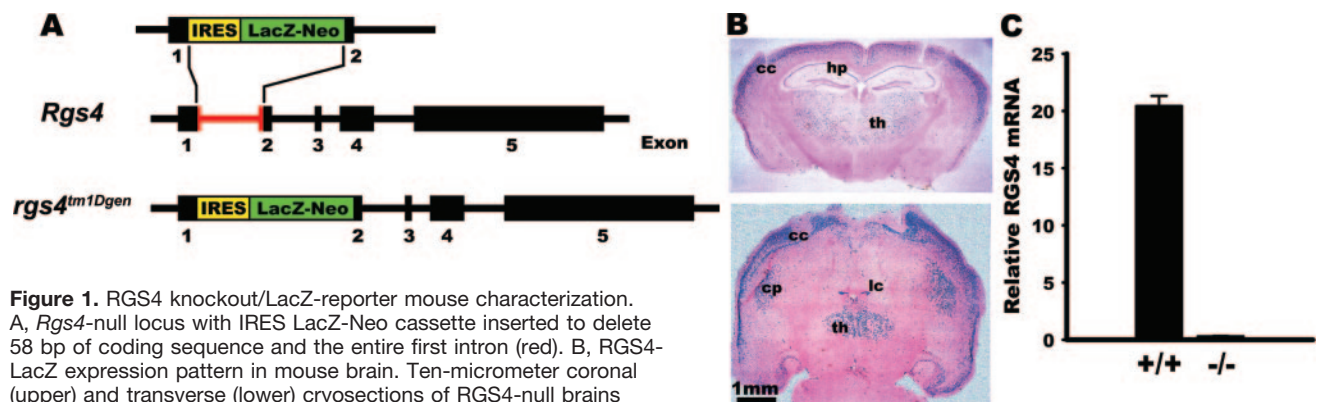


**Figure 1.** RGS4 knockout/LacZ-reporter mouse characterization. **A**, *Rgs4*-null locus with IRES LacZ-Neo cassette inserted to delete 58 bp of coding sequence and the entire first intron (red). **B**, RGS4-LacZ expression pattern in mouse brain. Ten-micrometer coronal (upper) and transverse (lower) cryosections of RGS4-null brains stained for LacZ show reporter gene expression in the cerebral cortex (cc), hippocampus (hp), thalamus (th), caudoputamen (cp), and locus coeruleus (lc). **C**, *Rgs4* deletion in brain tissue was verified by real-time PCR of total mRNA from the brains of wild-type (+/+) and *RGS4*-null (-/-) mice.  $\Delta C_T$  values were normalized to 18S and compared with RGS3 mRNA of +/+ hearts (as the calibrator sample), as described in the online data supplement. Data are representative of at least 3 independent experiments.

parasympathetic signaling in the SAN. RGS4 was originally believed to be brain-specific with its high expression in the cerebral cortex and thalamus.<sup>18</sup> Indeed motor memory defects have been identified in *RGS4*-deficient mice.<sup>19</sup> This study investigates a role for RGS4 in the regulation of the SAN by the parasympathetic system.

Here, we use a *RGS4* knockout mouse expressing LacZ behind the *Rgs4* promoter to show that *Rgs4* is highly expressed in the SAN. The discovery of increased parasympathetic-mediated signaling in *RGS4*-deficient animals, isolated hearts, and isolated SAN myocytes demonstrates that RGS4 is normally required for attenuation of parasympathetic-dependent G protein signaling in the SAN and intrinsic conduction system.

## Materials and Methods

An expanded Materials and Methods section is available in the online data supplement at <http://circres.ahajournals.org>.

### Animals

The *Rgs4<sup>tm1Dgen</sup>/J* mouse strain was obtained from The Jackson Laboratory (Bar Harbor, Maine, <http://jaxmice.jax.org/strain/005833.html>). Mice were backcrossed > six generations into a C57Bl/6 background.

### Statistical Analysis

Data are reported as means  $\pm$  SE. Data were analyzed using 1-way and 2-way ANOVA with Tukey's or Dunn's post hoc analysis and Student's *t* tests, as appropriate. In all instances,  $P < 0.05$  was considered significant.

## Results

### RGS4 Is Highly Expressed in the SAN

To characterize the role of RGS4 as a regulator of parasympathetic signaling in the SAN, we used *RGS4*-null mice expressing LacZ from the endogenous *Rgs4* promoter. The targeted locus produces a truncated, nonfunctional RGS4 protein lacking its RGS domain (Figure 1A). As shown in Figure 1B, LacZ expression patterns in the brains of *RGS4* heterozygous mice matched those previously reported for the endogenous RGS4 mRNA.<sup>18,19</sup> Real-time RT-PCR analysis

confirmed the loss of RGS4 mRNA in brains from knockout mice (Figure 1C).

Hearts from heterozygous animals showed an intense crescent-shaped pattern of LacZ staining on the exterior surface of the heart at the junction of the superior vena cava (SVC) and right atrium (Figure 2A, arrowheads), which is the region containing the SAN.<sup>20,21</sup> To more precisely identify the location of RGS4 expression, the atria were dissected off the heart and mounted to visualize the endocardial SAN region.<sup>22,23</sup> Low-magnification images revealed significant levels of RGS4 expression in the SAN and vasculature (Figure 2B). High magnification of this region showed the compact intense LacZ staining within the SVC-proximal region of the SAN extending toward the base of the right atrium (Figure 2C). LacZ expression was also observed, albeit at much lower levels in vascular smooth muscle cells and pericytes of the coronary vasculature. Notably, no LacZ expression was observed in working atrial myocardium, including the crista terminalis, and the right atrial appendage (RAA), Purkinje fibers, or in the working ventricular myocardium (data not shown). RT-PCR analysis of wild-type mice confirmed higher relative expression levels in SAN compared to RAAs (Figure 2D). To ensure our LacZ-stained regions corresponded to the SAN, immunohistochemistry for HCN4 (Figure 2F and Figure I in the online data supplement) was performed in parallel with LacZ staining (Figure 2E). These results revealed that *Rgs4* is highly and selectively coexpressed with pacemaker channels in the SAN.

### Enhanced Parasympathetic-Mediated HR Regulation in RGS4-Deficient Mice

Despite high levels of RGS4 expression in the SAN, basal heart rates (Figure 3A) and blood pressures (data not shown) in conscious *RGS4*-null mice were not different from wild-type mice (controls). However, consistent with a role for RGS4 in the regulation of M<sub>2</sub>R signaling in the SAN, *RGS4*-null animals showed markedly enhanced heart rate responses to systemically administered carbachol (carbamylcholine chloride [CCh]) (0.1 mg/kg IP), suggesting that RGS4 function is important when parasympathetic tone is increased. Notably, under anesthetized conditions, in which

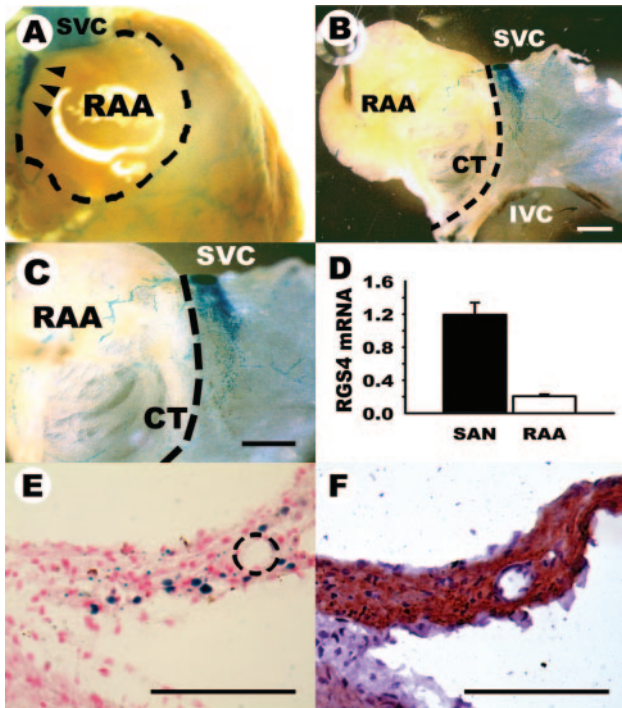


**Figure 2.** RGS4-LacZ reporter expression is high within SAN myocytes. A, Whole-mount intact heart showing intense LacZ expression observed in a crescent-shaped pattern within the right atrium at the base of the SVC (arrowheads) extending along the crista terminalis into the right atrium. Dashed border shows outline of RAA. B, Wide-angle view of an atrial preparation showing the atrial septum and RAA from RGS4-null mice stained for LacZ expression. SVC indicates superior vena cava; IVC, inferior vena cava; CT, crista terminalis. C, High-magnification view of a stained atrial preparation shows RGS4-LacZ expression in the SAN. Scale bars=1 mm. Dashed border in B and C shows border of CT and atrial septum. D, Comparison of RGS4 mRNA expression in the SAN and RAA from wild-type (WT) mice was carried out by real-time RT-PCR as described above. Parallel cross-sections (see supplemental Figure I) of the SAN region of the atrial preparation were stained for LacZ expression (E) and labeled by immunohistochemistry for the SAN-specific antigen HCN4 (red staining) (F). Images were collected at  $\times 40$  magnification. Black dashed circle in E indicates position of the sinoatrial node artery. Scale bars=100 micrometers.

increased parasympathetic tone is expected, RGS4-null mice showed reduced basal HR (Figure 4A) and reduced mean arterial pressures (data not shown) compared to wild-type controls. These differences in HR were abolished by the IV administration of atropine, a potent M<sub>2</sub>R antagonist. Specifically, atropine (0.3 mg/kg) had minimal effects on HR in wild-type animals, as expected from previous reports,<sup>24–26</sup> while inducing large HR increases in RGS4-null mice (Figure 4A and 4B). Importantly, atropine eliminated the HR differences between the groups. These data suggest that autonomic control of SAN activity is biased toward greater parasympathetic activity because of reduced inhibition of M<sub>2</sub>R-coupled G protein signaling in RGS4-null mice relative to controls.

### Increased Bradycardia in CCh-Treated RGS4-Deficient Hearts

It is conceivable that the results described above could be explained by differences in central nervous system activity or

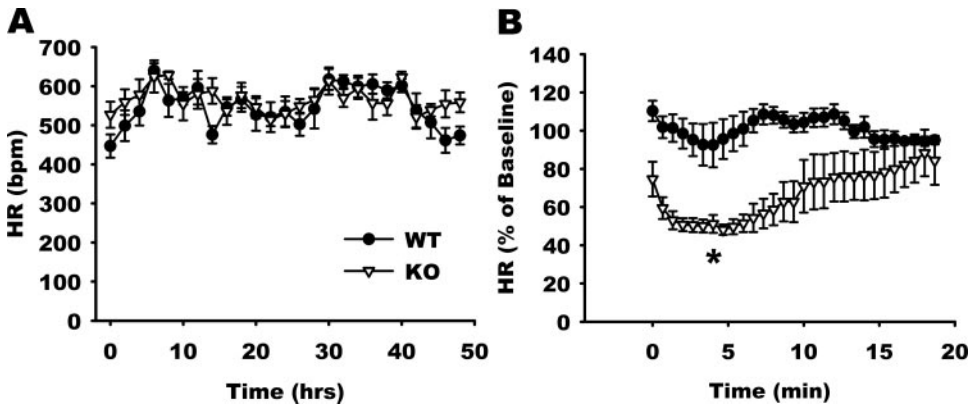
other neurohumoral factors between the groups of mice. To eliminate these differences, we studied isolated retrograde-perfused hearts. Although baseline HRs ( $\approx 430$  bpm) and ECG patterns of isolated hearts did not differ between genotypes (Figure 5A), CCh application dose-dependently reduced heart rates (estimated from R-R intervals) to a greater extent in RGS4-null hearts. In fact, at the highest dose of CCh tested (10  $\mu\text{mol/L}$ ), all RGS4-null hearts showed SAN standstill, whereas wild-type and heterozygous hearts were merely slowed but continued to beat (Figure 5A and 5B). All hearts showed complete recovery of the ECG trace following CCh washout (data not shown). Thus, the loss of RGS4 renders the SAN more sensitive to the bradycardic effects of the parasympathetic agonist CCh.

A separate group of isolated hearts was treated with 50 nmol/L isoproterenol (Iso) to mimic the in vivo conditions of high sympathetic tone before application of CCh. The response to sympathetic stimuli was not different between the groups, because wild-type and RGS4-deficient hearts had similar HRs ( $\approx 590$  bpm) after Iso treatment, with all hearts showing normal ECG patterns (supplemental Figure IIA). As with non-Iso-treated hearts, CCh application slowed HR in RGS4-null far more than in wild-type hearts (supplemental Figure IIB). Interestingly, however, CCh effects were more pronounced in both genotypes following pretreatment with Iso. For example, discernable P or QRS waves could not be detected in RGS4-null hearts (ie, the hearts were in SAN standstill) at CCh concentrations above 3  $\mu\text{mol/L}$ . Furthermore, RGS4-null hearts treated with Iso were more susceptible to atrioventricular node conduction block (ie, uncoupling of the P and QRS waves) and SAN standstill compared to nontreated hearts (supplemental Figure III and supplemental Table I). Together, these data suggest that RGS4 may modulate the previously reported crosstalk between  $\beta$ -adrenergic and M<sub>2</sub>R signaling.<sup>27</sup>

### Enhanced Effect of CCh on Spontaneous Action Potential Firing in RGS4-Deficient Mice

Next, we evaluated the role of RGS4 as a regulator of spontaneous action potential (AP) firing rates in cardiac pacemaker cells (Figure 6). AP frequency was not different between genotypes under basal conditions (176  $\pm$  12.6 bpm in wild-type myocytes versus 164.7  $\pm$  9.2 bpm in RGS4-null myocytes;  $P=0.93$ ). Superfusion of CCh (100 nmol/L) reduced AP frequency to 136  $\pm$  14.3 bpm in wild-type SAN myocytes, whereas in RGS4-null myocytes, AP frequency was profoundly reduced to 14.2  $\pm$  11.1 bpm (Figure 6A and 6B). Strikingly, AP firing was completely suppressed at this dose of CCh in 9 of 11 RGS4-null SAN myocytes. In contrast, no wild-type myocytes stopped firing spontaneous APs.

These changes in AP firing correlated with changes in the maximum diastolic potential (MDP) of the cells. Under basal conditions, MDP was  $-64.4 \pm 1.6$  mV in wild-type myocytes and  $-65.1 \pm 0.9$  mV in RGS4-null myocytes. CCh (100 nmol/L) hyperpolarized the MDP of wild-type cells to  $-67.1 \pm 1.6$  mV, whereas RGS4-null SAN myocytes were significantly more hyperpolarized to  $-73.6 \pm 0.9$  mV (Figure 6A and 6C). Although these effects of CCh on AP frequency and MDP were completely reversible on washout (Figure



was used to determine statistical significance of baselines and change in HR with CCh between groups. \* $P < 0.05$ .

6A), the time course of washout was significantly prolonged in RGS4-null SAN myocytes ( $151.0 \pm 6.6$  seconds) compared to wild-type myocytes ( $90.6 \pm 7.8$  seconds).

### $I_{K_{ACh}}$ Is Altered in Isolated Sinoatrial Myocytes From RGS4-Deficient Mice

The results above suggest that RGS4 regulates heart function by modulating parasympathetic-dependent signaling. The correlation between changes in AP frequency and MDP following application of CCh suggest that acetylcholine-activated  $K^+$  currents ( $I_{K_{ACh}}$ ),<sup>28</sup> produced by GIRK channels, are responsible for the altered parasympathetic signaling in RGS4-null mice. Thus, we measured  $I_{K_{ACh}}$  in isolated SAN myocytes. Figure 7A shows that application of CCh (10  $\mu$ mol/L) induces an increase in  $I_{K_{ACh}}$  (recorded at  $-100$  mV), which declines thereafter via a process referred to as desensitization.<sup>28</sup> Whereas peak  $I_{K_{ACh}}$  levels were similar between the groups, the time-dependent decline of  $I_{K_{ACh}}$  is reduced in RGS4-null myocytes relative to wild-type. Indeed, the extent of  $I_{K_{ACh}}$  desensitization (at  $-100$  mV) is less in RGS4-deficient ( $13.8 \pm 1.4\%$ ) compared to wild-type ( $30.4 \pm 2.1\%$ ) SAN myocytes (Figure 7B). The reduced desensitization in RGS4-null myocytes is also evident from the current/voltage relationship measured 2 minutes after CCh application (Figure 7D), which shows increased  $I_{K_{ACh}}$  in RGS4-null myocytes compared to control, without differences in peak  $I_{K_{ACh}}$  between the groups (Figure 7C). Consistent with the AP studies above, the decay kinetics of  $I_{K_{ACh}}$

following CCh removal (ie, the deactivation kinetics) were markedly delayed for RGS4-null myocytes during either CCh washout or the application of atropine to block  $M_2$ Rs (Figure 7E). Together, these data indicate prolonged  $G\alpha_{i/o}$  signaling in SAN myocytes following CCh removal, consistent with the known function of RGS4 as a GAP for  $G\alpha_{i/o}$ .<sup>8</sup> The delay in deactivation kinetics of  $I_{K_{ACh}}$  coincided with a corresponding slowing ( $P < 0.05$ ) of activation kinetics in RGS4-deficient SAN myocytes compared to wild-type SAN myocytes (Figure 7F). Kinetic slowing of the actions of CCh in the absence of RGS4 is also consistent with the previously identified role of RGS4 in accelerating the kinetics of the response of GIRK channels to  $G\alpha_{i/o}$  stimulation.<sup>16</sup> Thus, SAN myocytes from RGS4-null mice show markedly altered  $M_2$ R-dependent signaling characteristics and regulation of GIRK channel kinetics.

Finally, we evaluated the effects of 2 additional doses of CCh (1  $\mu$ mol/L and 100 nmol/L) on  $I_{K_{ACh}}$  to determine whether a component of the enhanced effect of parasympathetic signaling on HR regulation in RGS4-deficient hearts could be explained by a shift in the  $I_{K_{ACh}}$  dose-response curve. Figure 8A illustrates peak  $I_{K_{ACh}}$  current density at  $-100$  and  $+40$  mV. Peak currents were measured so that the maximal CCh response could be attained with minimal contribution from the desensitization effect. Despite a dose-dependent increase in peak  $I_{K_{ACh}}$  density in both genotypes, no differences in peak  $I_{K_{ACh}}$  density were observed between wild-type and RGS4-null SAN myocytes at any of the CCh doses

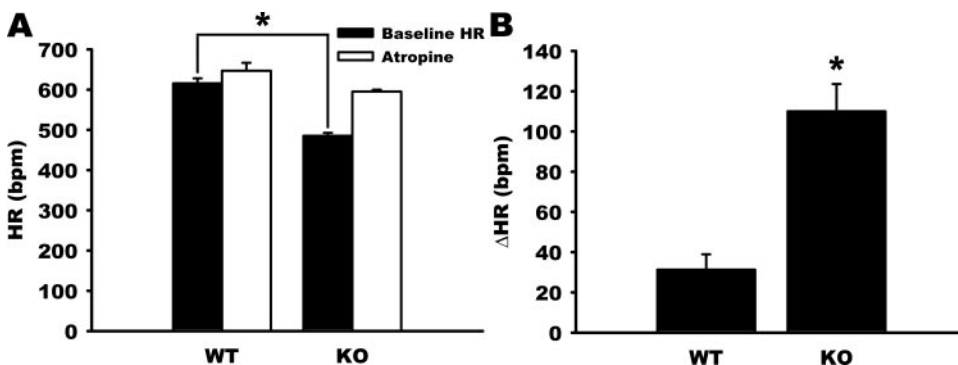


**Figure 4.** Atropine-dependent positive chronotropic effects are enhanced in RGS4-null mice compared with wild-type littermate controls. Heart rates of *Rgs4* wild-type ( $n=4$ ) and null (KO) ( $n=4$ ) mice were recorded with a Millar 1.4 F blood pressure catheter inserted into the common carotid artery. A, Basal (black bars) and atropine-stimulated (0.3 mg/kg) (white bars) HR were recorded. B, The change in HR from baseline levels following atropine administration

was determined. One-way ANOVA with a Tukey's HSD post hoc test was used to determine statistical significance of baselines and change in HR with atropine between groups. \* $P < 0.005$ .

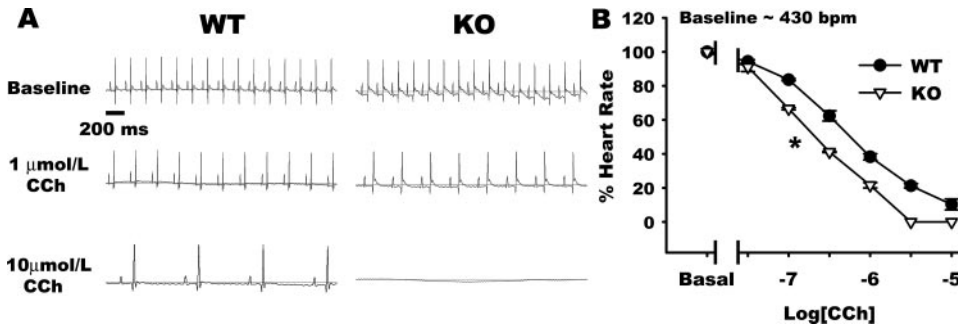


**Figure 5.** Increased negative chronotropy in isolated retrograde-perfused RGS4-null hearts. A, Representative ECG traces of isolated RGS4-null (KO) and wild-type hearts at baseline, and 1 and 10 μmol/L CCh. KO hearts show enhanced negative chronotropic effect at 1 μmol/L CCh and complete loss of the ECG at 10 μmol/L CCh compared to wild-type hearts. M<sub>2</sub>R-mediated negative

chronotropic responses are more pronounced in hearts isolated from RGS4-null (KO) compared to wild-type littermate control mice (n=5 hearts for wild-type and n=5 hearts for KO). B, Beating rate (BR) was determined from the R-R intervals of an ECG trace. The effect of increasing concentrations of the M<sub>2</sub>R agonist CCh was examined. Average BRs were expressed as a percentage of the 30-minute baseline BR. Trace amplitudes are normalized for comparison. ANOVA with a Tukey's HSD post hoc was used to determine statistical significance. \*P<0.005.

tested. By contrast, the extent of I<sub>KACH</sub> desensitization following a 2-minute application of CCh at concentrations of 10 μmol/L (Figure 7B) and 1 μmol/L and 100 nmol/L (Figure 8B) was less for RGS4-deficient compared to wild-type myocytes at all concentrations tested. Notably, the greatest relative difference in the percentage of desensitization occurred at 100 nmol/L (Figure 8C), consistent with a role for potent regulation of GIRK activity by RGS4 at physiological M<sub>2</sub>R agonist concentrations.<sup>22</sup> This may explain the dose-dependent differences in HR in the response to CCh between the genotypes. Together, these data suggest that enhanced CCh signaling in the SAN of RGS4-null mice is the

result of altered I<sub>KACH</sub> desensitization and kinetics rather than a shift in the dose response.

**Discussion**

Previous studies showed that RGS4 mRNA is expressed in atrial<sup>11,12,27</sup> and ventricular<sup>12,29</sup> myocytes; however, its expression in the murine SAN has not been examined previously. Using 2 approaches (ie, LacZ reporter/HCN4 immunostaining colocalization and real-time RT-PCR), our results demonstrate that RGS4 is more highly expressed in SAN myocytes compared to myocytes in the RAA. Because RGS4 is known to attenuate Gα<sub>i/o</sub> but not Gα<sub>s</sub> activation, we

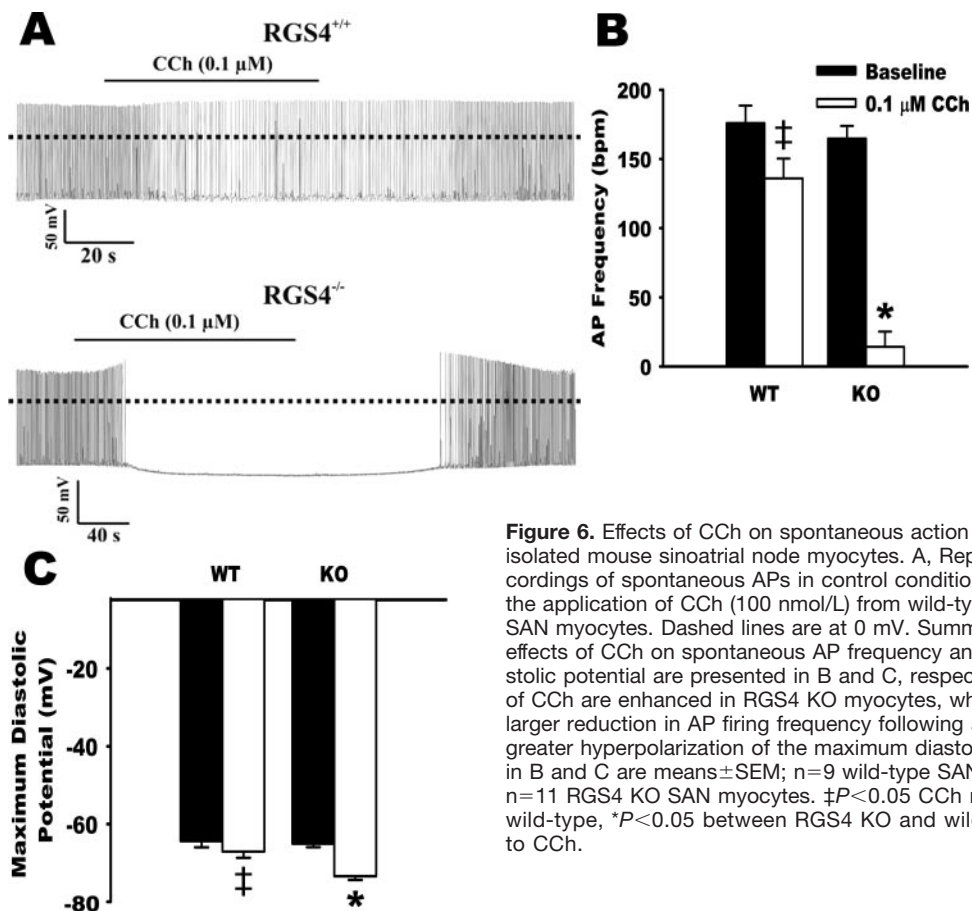


**Figure 6.** Effects of CCh on spontaneous action potential firing in isolated mouse sinoatrial node myocytes. A, Representative recordings of spontaneous APs in control conditions and following the application of CCh (100 nmol/L) from wild-type and RGS4 KO SAN myocytes. Dashed lines are at 0 mV. Summary data for the effects of CCh on spontaneous AP frequency and maximum diastolic potential are presented in B and C, respectively. The effects of CCh are enhanced in RGS4 KO myocytes, which results in a larger reduction in AP firing frequency following a significantly greater hyperpolarization of the maximum diastolic potential. Data in B and C are means±SEM; n=9 wild-type SAN myocytes and n=11 RGS4 KO SAN myocytes. †P<0.05 CCh response within wild-type, \*P<0.05 between RGS4 KO and wild-type response to CCh.

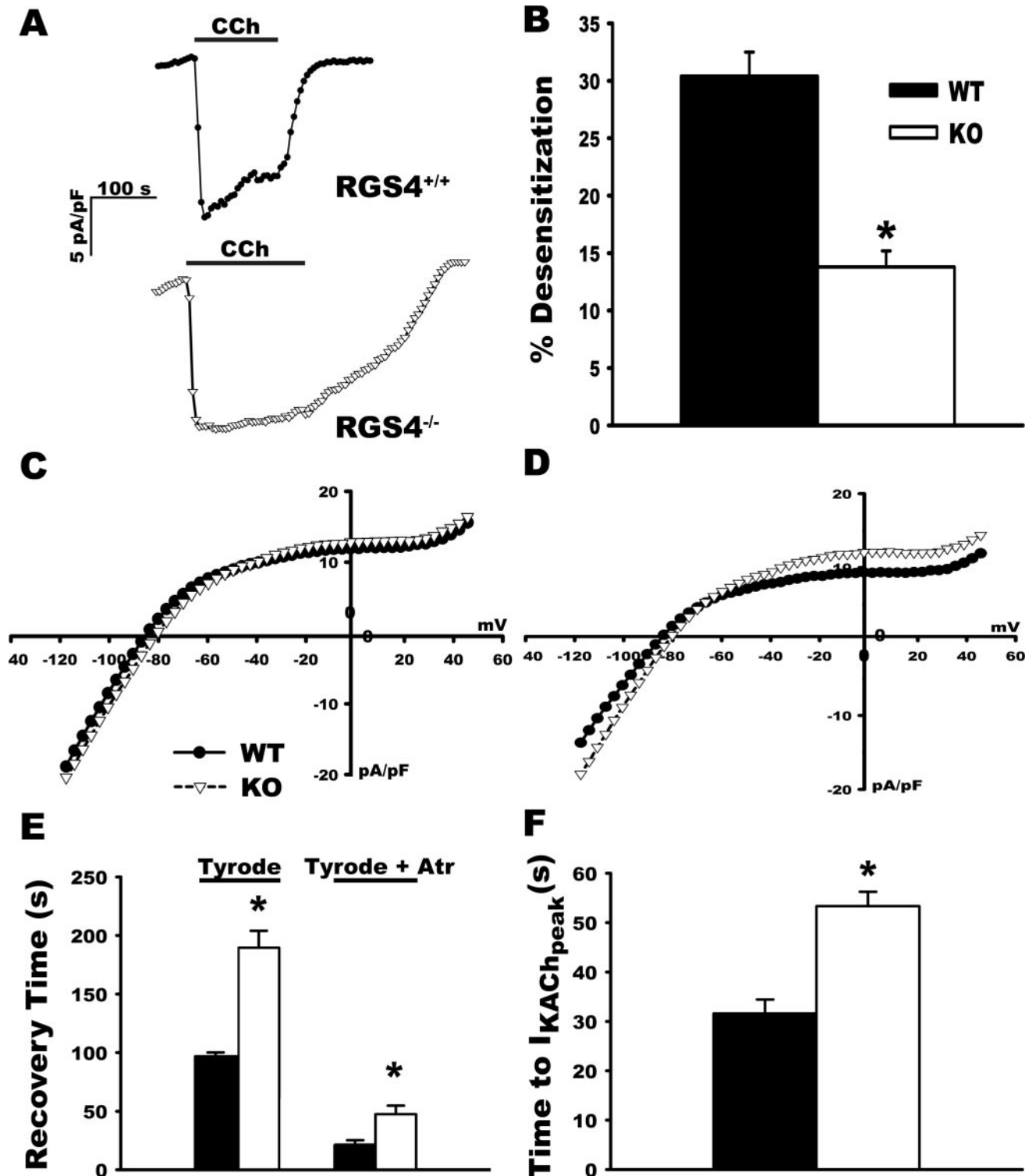


**Figure 7.** Effect of RGS4-deficiency on  $M_2R$ -evoked GIRK currents ( $I_{KACH}$ ) in isolated wild-type ( $\bullet$ ;  $n=26$ ) and RGS4-null (KO) ( $\nabla$ ;  $n=19$ ) SAN myocytes. **A**, Representative  $I_{KACH}$  traces show the effect of  $10 \mu\text{mol/L}$  CCh application and washout on GIRK channel activity in wild-type and KO cells. KO myocytes show decreased desensitization to CCh treatment compared to wild-type cells. **B**,  $I_{KACH}$  desensitization to  $10 \mu\text{mol/L}$  CCh was determined as the percentage of the peak current remaining following 2 minute treatment with CCh as in **A** above. Shown are the mean values derived from wild-type and KO cells. **C** and **D**,  $I_{KACH}$  current–voltage relationships were investigated at the time of peak current (**C**) and after 2-minute CCh treatment (**D**) using a voltage ramp from  $+50$  to  $-120$  mV (holding potential was  $-75$  mV). Data represent the mean current values. **E** and **F**, Effect of loss of RGS4 function on the temporal modulation of  $I_{KACH}$ . Shown are the mean time for  $I_{KACH}$  deactivation (**E**) and activation (**F**) following CCh washout and application, respectively. KO SAN myocytes show prolonged  $I_{KACH}$  deactivation kinetics on removal of CCh and prolonged  $I_{KACH}$  activation kinetics compared to wild-type SAN myocytes. ANOVA was used with Dunn’s multiple comparison procedure or paired and unpaired Student’s  $t$  tests, as appropriate. \* $P < 0.05$  compared to wild-type.

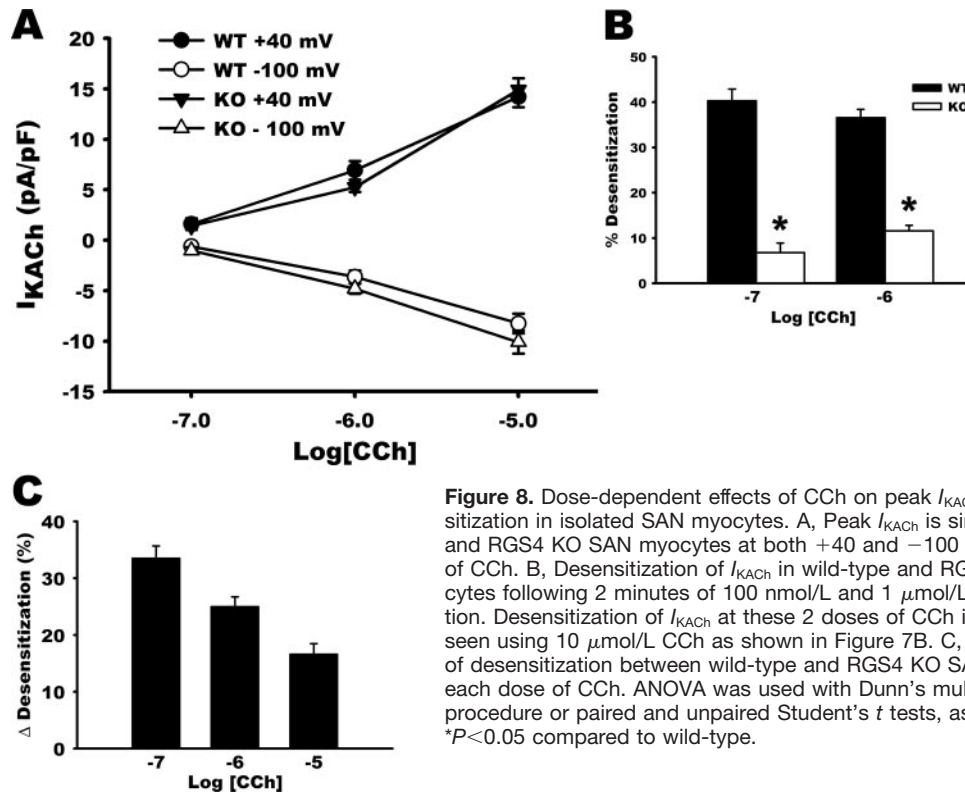


**Figure 8.** Dose-dependent effects of CCh on peak  $I_{KACH}$  and  $I_{KACH}$  desensitization in isolated SAN myocytes. **A**, Peak  $I_{KACH}$  is similar in wild-type and RGS4 KO SAN myocytes at both +40 and -100 mV, at each dose of CCh. **B**, Desensitization of  $I_{KACH}$  in wild-type and RGS4KO SAN myocytes following 2 minutes of 100 nmol/L and 1  $\mu$ mol/L CCh administration. Desensitization of  $I_{KACH}$  at these 2 doses of CCh is similar to that seen using 10  $\mu$ mol/L CCh as shown in Figure 7B. **C**, Difference in level of desensitization between wild-type and RGS4 KO SAN myocytes at each dose of CCh. ANOVA was used with Dunn's multiple comparison procedure or paired and unpaired Student's *t* tests, as appropriate. \**P*<0.05 compared to wild-type.

anticipated that its loss would cause selective increases in the response to parasympathetic stimulation in the SAN. Basal HRs in conscious RGS4-deficient mice were not different from wild-type controls, potentially because of the dominant effect of sympathetic versus parasympathetic tone on HR control in mice. However, consistent with a role for RGS4 in the regulation of HR under conditions of increased parasympathetic tone, conscious RGS4-deficient mice showed enhanced bradycardic responses to CCh and anesthetized RGS4-deficient animals showed lower basal HR levels. Atropine-mediated normalization of HR levels in the latter model supported the notion that increased parasympathetic activity could regulate RGS4-null hearts to a greater extent than wild-type. Although it is conceivable that the altered HR regulation in RGS4-null mice is partially attributable to the loss of RGS4 in the central nervous system and/or coronary vasculature, it seems likely that an enhanced intrinsic responsiveness of SAN myocytes to vagal stimulation plays a significant role. Enhanced intrinsic sensitivity of the SAN to vagal stimulation is also supported by the observation that isolated RGS4-deficient hearts showed enhanced bradycardia in response to the M<sub>2</sub>R agonist CCh. In fact, the RGS4-deficient hearts were so sensitive to the application of CCh that they experienced SAN standstill at doses of 3  $\mu$ mol/L. Thus, it seems likely that loss of RGS4 in the SAN dramatically sensitizes these hearts to parasympathetic activity at the level of HR depression.

Because M<sub>2</sub>R is selectively coupled to the G $\alpha_{i/o}$  subclass of heterotrimeric G proteins, it is likely that the majority of M<sub>2</sub>R-mediated responses in the SAN are mediated by signaling through G $\alpha_{i/o}$  and its effectors. Additionally, because RGS proteins are potent inhibitors of G $\alpha_{i/o}$  function at the

plasma membrane, we expect that the loss of RGS proteins will increase G $\alpha_{i/o}$  signaling in SAN myocytes. Although a number of end effectors in SAN myocytes could transduce the G $\alpha_{i/o}$ -mediated signals to produce the lower HRs observed in RGS4-deficient mice, we focused on comparing  $I_{KACH}$  between the different mouse groups because of the observed changes in MDP during spontaneous AP firing (Figure 6) and the prominent role that this current plays in mediating HR slowing in response to vagal stimulation.<sup>30</sup> Moreover, RGS4 is known to modulate GIRK channel function in heterologous expression systems.<sup>17,31,32</sup> Consistent with an increased level of G $\alpha_{i/o}$  signaling, CCh-treated SAN myocytes from RGS4-deficient mice showed increased  $I_{KACH}$  as a result of reduced desensitization and altered GIRK gating kinetics. However, because RGS4 functions at the receptor level to inhibit all G $\alpha_{i/o}$ -mediated signaling, it is possible that other pathways regulated by parasympathetic stimuli, including adenylyl cyclase activity, phosphodiesterase activity, intracellular cyclic nucleotide levels, protein kinase A activity, HCN, and L-type calcium channels,<sup>2-4</sup> may also be altered in RGS4-null hearts.

This is the first demonstration that RGS4 is required for rapid desensitization of GIRK-mediated  $I_{KACH}$  in the SAN. These data suggest that RGS4 is part of a negative feedback regulatory mechanism for activated M<sub>2</sub>R-G $\alpha_{i/o}$ -GIRK complexes. Previous work to define the mechanisms of GIRK desensitization suggested desensitization was resolved into fast and slow phases, where the fast phase is explained by  $I_{KACH}$  channel dephosphorylation<sup>33</sup> and RGS protein GAP activity<sup>34</sup> and the slow phase involves G protein receptor kinase activity.<sup>35,36</sup> Because RGS4 has not been implicated in the regulation of kinases or phosphatases in the cell, the loss

of rapid phase desensitization in RGS4-deficient SAN myocytes likely indicates the loss of a GAP-dependent desensitization mechanism. It has been shown that RGS4 forms stable protein–protein interactions with both M<sub>2</sub>R<sup>14</sup> and GIRK3<sup>15</sup> channels, and, thus, it is proposed to be a component of an integrated kinetic scaffolding complex that promotes efficient coordinated regulation of both G protein and GIRK activation.<sup>37</sup> Consistent with the reported effects of RGS4 on the kinetic regulation of G $\alpha_{i/o}$ -mediated modulation of GIRK channels,  $I_{K_{ACh}}$  measured in SAN myocytes lacking RGS4 showed slower activation and deactivation compared to wild-type cells. Taken together, these data provide strong evidence for defective G $\alpha_{i/o}$  signaling and GIRK regulation in SAN myocytes lacking a selective G $\alpha_{i/o}$  GAP and point to the possibility that RGS4 plays a role in parasympathetic regulation of beat-to-beat changes in intact animals.

These data raise the possibility that reduction of RGS4 expression or function in a pathophysiological setting could increase susceptibility to bradycardia and arrhythmia. It is interesting that, like the RGS-resistant G $\alpha_1$ - or G $\alpha_o$ -expressing mice, RGS4-null mice do not show increased vagal-mediated effects on baseline HR in vivo,<sup>9</sup> perhaps reflecting an increased level of sympathetic drive in the murine models. Future studies will determine whether RGS4 is critical for SAN regulation under basal conditions in humans, who normally have higher intrinsic levels of parasympathetic tone.

In addition to showing a chronotropic phenotype, RGS-resistant G $\alpha_{i2}$  mice showed slowed conduction through the atrioventricular node and susceptibility to atrioventricular block and other conduction defects.<sup>10</sup> Similarly, Iso-treated hearts from mice lacking RGS4 show M<sub>2</sub>R-dependent atrioventricular node block and cardiac arrest, implicating its potential role as a regulator of the crosstalk mechanisms between  $\beta$ -adrenergic receptors and M<sub>2</sub>R.<sup>27</sup> However, it remains to be determined whether atrioventricular node conduction is altered in RGS4-deficient mice and whether loss of RGS4 in regions of the heart outside of the SAN significantly increases the susceptibility of hearts to conduction defects and arrhythmogenesis in vivo.

In summary, we show that RGS4 modulates the G $\alpha_{i/o}$ -mediated regulation of cardiac automaticity, leading to enhanced bradycardic responses following M<sub>2</sub>R activation in RGS4-deficient mice. Moreover, the conduction defects associated with dysregulation of G $\alpha_{i/o}$ -mediated activation of GIRK channels and other parasympathetic effectors suggest that RGS4 may normally provide protection from arrhythmogenic stimuli. Indeed, it has been shown that GIRK4 knockout mice and mice with altered expression of G $\beta$  subunits exhibited significantly reduced HR variability and a reduced propensity for atrial fibrillation.<sup>38,39</sup> Because increases in parasympathetic activity is associated with susceptibility to cardiac arrhythmias,<sup>6</sup> conditions that lead to loss of RGS4 function might be expected to increase the probability of arrhythmia and atrial fibrillation. Accordingly, it will be of interest to characterize the expression and function of RGS4 in sick sinus syndrome and heart failure in humans. In the future, the search for compounds that increase both the expression and function of RGS4 may provide a valuable

therapeutic strategy for the treatment and prevention of heart disease.

## Acknowledgments

We acknowledge technical support from the Cell Biology of Atherosclerosis Group at the University of Toronto, with special thanks to Drs Philip Marsden and Michelle Bendeck for assistance with real-time RT-PCR and histological analysis.

## Sources of Funding

Technical and financial assistance for this work was provided by the Heart & Stroke/Richard Lewar Centre of Excellence (HSRLCE) in Cardiovascular Research. This work was supported by Heart and Stroke Foundation of Ontario Grant-in-Aid Program grants NA5921/T5835 (to S.P.H.) and operating grants from the Canadian Institutes of Health Research (MOP-68965 to P.H.B.). Career support came from the Canada Research Chairs Program (S.P.H.), the Heart & Stroke Foundation of Ontario Career Investigator Program (P.H.B.), the Canadian Institutes of Health Research–Tailored Advanced Collaborative Training in Cardiovascular Science program (R.A.R.) and Canadian Institutes of Health Research–Canada Graduate Scholarship Program (C.C.), and the Alberta Heritage Foundation for Medical Research (R.A.R.).

## Disclosures

None.

## References

- DiFrancesco D. Funny channels in the control of cardiac rhythm and mode of action of selective blockers. *Pharmacol Res.* 2006;53:399–406.
- Irisawa H, Brown HF, Giles W. Cardiac pacemaking in the sinoatrial node. *Physiol Rev.* 1993;73:197–227.
- Kubo Y, Reuveny E, Slesinger PA, Jan YN, Jan LY. Primary structure and functional expression of a rat G-protein-coupled muscarinic potassium channel. *Nature.* 1993;364:802–806.
- DiFrancesco D. Pacemaker mechanisms in cardiac tissue. *Annu Rev Physiol.* 1993;55:455–472.
- Fischmeister R, Castro LR, Abi-Gerges A, Rochais F, Jurevicius J, Leroy J, Vandecasteele G. Compartmentation of cyclic nucleotide signaling in the heart: the role of cyclic nucleotide phosphodiesterases. *Circ Res.* 2006;99:816–828.
- Dobrzynski H, Boyett MR, Anderson RH. New insights into pacemaker activity: promoting understanding of sick sinus syndrome. *Circulation.* 2007;115:1921–1932.
- Watson N, Linder ME, Druey KM, Kehrl JH, Blumer KJ. RGS family members: GTPase-activating proteins for heterotrimeric G-protein alpha-subunits. *Nature.* 1996;383:172–175.
- Berman DM, Wilkie TM, Gilman AG. GAIP and RGS4 are GTPase-activating proteins for the Gi subfamily of G protein alpha subunits. *Cell.* 1996;86:445–452.
- Fu Y, Huang X, Zhong H, Mortensen RM, D'Alecy LG, Neubig RR. Endogenous RGS proteins and Galpha subtypes differentially control muscarinic and adenosine-mediated chronotropic effects. *Circ Res.* 2006;98:659–666.
- Fu Y, Huang X, Piao L, Lopatin AN, Neubig RR. Endogenous RGS proteins modulate SA and AV nodal functions in isolated heart: implications for sick sinus syndrome and AV block. *Am J Physiol Heart Circ Physiol.* 2007;292:H2532–H2539.
- Doupnik CA, Xu T, Shinaman JM. Profile of RGS expression in single rat atrial myocytes. *Biochim Biophys Acta.* 2001;1522:97–107.
- Kardstun T, Wu H, Lim AL, Neer EJ. Cardiac myocytes express mRNA for ten RGS proteins: changes in RGS mRNA expression in ventricular myocytes and cultured atria. *FEBS Lett.* 1998;438:285–288.
- Wieland T, Mittmann C. Regulators of G-protein signalling: multifunctional proteins with impact on signalling in the cardiovascular system. *Pharmacol Ther.* 2003;97:95–115.
- Jaen C, Doupnik CA. RGS3 and RGS4 differentially associate with G protein-coupled receptor-Kir3 channel signaling complexes revealing two modes of RGS modulation. Precoupling and collision coupling. *J Biol Chem.* 2006;281:34549–34560.

15. Fujita S, Inanobe A, Chachin M, Aizawa Y, Kurachi Y. A regulator of G protein signalling (RGS) protein confers agonist-dependent relaxation gating to a G protein-gated K<sup>+</sup> channel. *J Physiol.* 2000;526:341–347.
16. Doupnik CA, Davidson N, Lester HA, Kofuji P. RGS proteins reconstitute the rapid gating kinetics of gbetagamma-activated inwardly rectifying K<sup>+</sup> channels. *Proc Natl Acad Sci U S A.* 1997;94:10461–10466.
17. Doupnik CA, Jaen C, Zhang Q. Measuring the modulatory effects of RGS proteins on GIRK channels. *Methods Enzymol.* 2004;389:131–154.
18. Gold SJ, Ni YG, Dohlman HG, Nestler EJ. Regulators of G-protein signaling (RGS) proteins: region-specific expression of nine subtypes in rat brain. *J Neurosci.* 1997;17:8024–8037.
19. Grillet N, Pattyn A, Contet C, Kieffer BL, Goridis C, Brunet JF. Generation and characterization of Rgs4 mutant mice. *Mol Cell Biol.* 2005;25:4221–4228.
20. Liu J, Dobrzynski H, Yanni J, Boyett MR, Lei M. Organisation of the mouse sinoatrial node: structure and expression of HCN channels. *Cardiovasc Res.* 2007;73:729–738.
21. Boyett MR, Honjo H, Kodama I. The sinoatrial node, a heterogeneous pacemaker structure. *Cardiovasc Res.* 2000;47:658–687.
22. Mangoni ME, Nargeot J. Properties of the hyperpolarization-activated current (I<sub>f</sub>) in isolated mouse sino-atrial cells. *Cardiovasc Res.* 2001;52:51–64.
23. Rose RA, Lomax AE, Kondo CS, nand-Srivastava MB, Giles WR. Effects of C-type natriuretic peptide on ionic currents in mouse sinoatrial node: a role for the NPR-C receptor. *Am J Physiol Heart Circ Physiol.* 2004;286:H1970–H1977.
24. Gehrman J, Hammer PE, Maguire CT, Wakimoto H, Triedman JK, Berul CI. Phenotypic screening for heart rate variability in the mouse. *Am J Physiol Heart Circ Physiol.* 2000;279:H733–H740.
25. Jumrussirikul P, Dinerman J, Dawson TM, Dawson VL, Ekelund U, Georgakopoulos D, Schramm LP, Calkins H, Snyder SH, Hare JM, Berger RD. Interaction between neuronal nitric oxide synthase and inhibitory G protein activity in heart rate regulation in conscious mice. *J Clin Invest.* 1998;102:1279–1285.
26. Just A, Faulhaber J, Ehmke H. Autonomic cardiovascular control in conscious mice. *Am J Physiol Regul Integr Comp Physiol.* 2000;279:R2214–R2221.
27. Bender K, Nasrollahzadeh P, Timpert M, Liu B, Pott L, Kienitz MC. A role for RGS10 in beta-adrenergic modulation of G-protein-activated K<sup>+</sup> (GIRK) channel current in rat atrial myocytes. *J Physiol.* 2008;586:2049–2060.
28. Lomax AE, Rose RA, Giles WR. Electrophysiological evidence for a gradient of G protein-gated K<sup>+</sup> current in adult mouse atria. *Br J Pharmacol.* 2003;140:576–584.
29. Mittmann C, Chung CH, Hoppner G, Michalek C, Nose M, Schuler C, Schuh A, Eschenhagen T, Weil J, Pieske B, Hirt S, Wieland T. Expression of ten RGS proteins in human myocardium: functional characterization of an upregulation of RGS4 in heart failure. *Cardiovasc Res.* 2002;55:778–786.
30. Wickman K, Nemecek J, Gendler SJ, Clapham DE. Abnormal heart rate regulation in GIRK4 knockout mice. *Neuron.* 1998;20:103–114.
31. Zhang Q, Pacheco MA, Doupnik CA. Gating properties of GIRK channels activated by Galpha (o)- and Galpha (i)-coupled muscarinic m2 receptors in *Xenopus* oocytes: the role of receptor precoupling in RGS modulation. *J Physiol.* 2002;545:355–373.
32. Zhang Q, Dickson A, Doupnik CA. Gbetagamma-activated inwardly rectifying K<sup>+</sup> (GIRK) channel activation kinetics via Galphai and Galphao-coupled receptors are determined by Galpha-specific inter-domain interactions that affect GDP release rates. *J Biol Chem.* 2004;279:29787–29796.
33. Shui Z, Boyett MR, Zang WJ. ATP-dependent desensitization of the muscarinic K<sup>+</sup> channel in rat atrial cells. *J Physiol.* 1997;505:77–93.
34. Chuang HH, Yu M, Jan YN, Jan LY. Evidence that the nucleotide exchange and hydrolysis cycle of G proteins causes acute desensitization of G-protein gated inward rectifier K<sup>+</sup> channels. *Proc Natl Acad Sci U S A.* 1998;95:11727–11732.
35. Shui Z, Boyett MR, Zang WJ, Haga T, Kameyama K. Receptor kinase-dependent desensitization of the muscarinic K<sup>+</sup> current in rat atrial cells. *J Physiol.* 1995;487:359–366.
36. Shui Z, Khan IA, Tsuga H, Haga T, Boyett MR. Role of receptor kinase in short-term desensitization of cardiac muscarinic K<sup>+</sup> channels expressed in Chinese hamster ovary cells. *J Physiol.* 1998;507:325–334.
37. Benians A, Nobles M, Hosny S, Tinker A. Regulators of G-protein signaling form a quaternary complex with the agonist, receptor, and G-protein. A novel explanation for the acceleration of signaling activation kinetics. *J Biol Chem.* 2005;280:13383–13394.
38. Gehrman J, Meister M, Maguire CT, Martins DC, Hammer PE, Neer EJ, Berul CI, Mende U. Impaired parasympathetic heart rate control in mice with a reduction of functional G protein betagamma-subunits. *Am J Physiol Heart Circ Physiol.* 2002;282:H445–H456.
39. Kovoov P, Wickman K, Maguire CT, Pu W, Gehrman J, Berul CI, Clapham DE. Evaluation of the role of I(KACh) in atrial fibrillation using a mouse knockout model. *J Am Coll Cardiol.* 2001;37:2136–2143.

## MATERIALS AND METHODS

### Animals

All experiments conformed to the Guide for the Care and Use of Laboratory Animals published by the US National Institutes of Health (NIH Publication No. 85-23, revised 1996), Institutional Guidelines and the Canadian Council on Animal Care.

### qRT-PCR Reaction and Quantitative Analysis

Total RNA was extracted from tissues using TRIzol reagent (Invitrogen Life Technologies). All quantitative RT-PCR was performed using an ABI Prism 7900 HT (Applied Biosystems) using the Sybr Green detection system. Two micrograms of total RNA was reverse transcribed with random hexamer primers using the Superscript II kit (Invitrogen Life Technologies) following the manufacturers protocols. cDNA was diluted to a final volume of 280 microliters. Two microliters of the RT reaction mixture was subsequently used as a template for real time PCR quantification. RGS primers used in this study were previously described and designed by Kurrasch *et al*<sup>1</sup>. Each cDNA sample was evaluated for RGS target genes of interest and two housekeeping genes, GAPDH and 18S, to serve as normalizing controls in independent wells. The following 5' PCR primers were used as the housekeeping genes.; GAPDH upstream, 5'-TTCACCACCATGGAGAAGG-3'; GAPDH downstream, 5'-CTCGTGGTTCACACCCATC-3'; 18S upstream, 5'-AGGAATTGACGGAAGGGCAC-3'; 18S downstream, 5'-GGACATCTAAGGGCATCACA-3'. A no-RT and no template control sample were included for each primer set. Data obtained from the PCR reaction were analyzed using the comparative  $C_T$  method (User Bulletin No. 2, Perkin Elmer Life Sciences). The  $C_T$  for each sample was manipulated first to determine the  $\Delta C_T$  [(average  $C_T$  of sample triplicates for the gene of interest) – (average  $C_T$  of sample triplicates for the normalizing gene)] and second to determine the  $\Delta\Delta C_T$  [ $\Delta C_T$  sample)–( $\Delta C_T$  for the calibrator sample)]. The internal calibrator sample (RGS3 mRNA in heart) was run concurrently on the same plate and designated as an external control, which was the sample showing the lowest expression level (highest  $\Delta C_T$ ). Values are expressed in log scale and the relative mRNA levels are established by conversion to a linear value using  $2^{-\Delta\Delta C_T}$ . Data represent the relative mRNA levels for each RGS in these tissues.

### Analysis of $\beta$ -Galactosidase Gene Expression.

For detection of reporter gene expression in whole mount tissues, hearts or atria were excised and immersed in 4% paraformaldehyde for 30 minutes at room temperature. Tissues were incubated overnight at 37°C in PBS containing 5 mmol/L  $K_4Fe(CN)_6 \cdot 3H_2O$ , 5 mmol/L  $K_3Fe(CN)_6$ , 2 mmol/L  $MgCl_2$ , 0.02% Nonidet P-40, 0.01% SDS, and 1 mg/mL 4-chloro-5-bromom-3-indolyl- $\beta$ -galactopyranoside (X-Gal). Images of whole mount tissues were collected using a Leica DFC280 with Leica Applications Suite software (Version 2.4.0R1) (Leica Microsystems, Switzerland).

### Cryosectioning of LacZ stained tissues.

Samples were equilibrated 30% sucrose (weight/volume) and immersed in OCT compound before freezing in dry ice cooled isopentane. Cryosections (8 to 10 micron) were mounted on surface-treated glass slides, postfixed briefly, stained with nuclear fast red and photographed on a Nikon Eclipse E-600 dissecting microscope and a Hamamatsu Digital Camera C4742-95 and

Simple PCI Version 5.3.0.1102 (Compix, Inc Imaging Systems). In brain and atrial preparation samples, cryosectioning preceded LacZ and counterstaining.

### **Immunohistochemistry**

Atrial cryosections were stained with an HCN4 antibody as previously done by Liu *et al.*<sup>2</sup>, to determine that RGS4 is highly expressed in the sinus region. Briefly, frozen serial sections (8–10  $\mu\text{m}$  thickness) were cut perpendicular to the crista terminalis from the top to the bottom of the preparations, and mounted on glass slides. Sections were incubated with anti-HCN4 IgG raised against residues 119–155 of human HCN4 (1:100 dilution; Alomone Labs) in 1% BSA at 4°C overnight. Following 2 hour room temperature incubation with a horseradish peroxidase-coupled goat anti-rabbit IgG secondary antibody, sections were stained by an immunoperoxidase kit (Vectastain, Avidin:Biotinylated enzyme complex kit PK-4000, Vector NovaRED peroxidase substrate, SK-4800, Vector Laboratories) according to the manufacturer's instructions. Tissue sections were counterstained with hemotoxylin, dehydrated, and mounted on microscope slides. Adjacent sections, one stained for LacZ and the following stained for HCN4, were compared.

### **Waking heart rate blood pressure measurements by radiotelemetry**

Heart rate was continuously monitored in waking unrestrained mice using radiotelemetry. Implantable mouse pressure and activity transmitters were from Data Sciences International (PhysioTel PA-C10). Prior to implantation, pressure transmitters were calibrated at three physiologic pressures (0, 50, and 100 mmHg) using a mercury manometer. One week prior to the start of the experiment, pressure catheters were surgically implanted into the aorta via the right carotid artery, and through the same ventral neck incision, a subcutaneous pouch is formed for placement of the transmitter itself along the animal's left flank. Following 48 baseline heart rate measurement, mice were injected IP with 0.1 mg/kg CCh and monitored for 20 min. Pressure and activity waveforms were acquired with Dataquest A.R.T Gold Acquisition version 4.1, and data were analyzed using Dataquest A.R.T Gold Analysis version 4.1.

### **In vivo heart rate measurement of anesthetized mice**

Mean arterial pressures (MAPs) and heart rates of isoflurane-anesthetized mice (1%) were recorded as described previously<sup>3</sup>. Atropine was administered (5  $\mu\text{l}$  doses added at a rate of 1–2  $\mu\text{l/s}$ ) via the left jugular vein using polyethylene tubing (PE-10) attached to a 1 ml syringe. Data are presented as mean values obtained from three to four mice, which were analyzed for statistical significance using one-way ANOVA and a Tukey's HSD post hoc test.

### **Isolated Heart Perfusion**

Mice were administered 1 mg/ml of heparin, sacrificed and the hearts were rapidly excised and rinsed in ice-cold modified Tyrodes solution [consisting of (in mmol/L) 118 NaCl, 5.4 KCl, 1 MgCl<sub>2</sub>, 1 NaH<sub>2</sub>PO<sub>4</sub>, 20 NaHCO<sub>3</sub>, 10 glucose, 0.5 pyruvate, and 1 CaCl<sub>2</sub>; pH 7.35]. Hearts were mounted on a perfusion apparatus for retrograde aortic perfusion with Tyrode's solution oxygenated with 95% O<sub>2</sub>-5% CO<sub>2</sub>, pH 7.3–7.4 at 37 °C] at a constant flow rate of 2.79 mL/min and allowed to stabilize for 20 min. Hearts with signs of ischemia, physical damage, persistent arrhythmia over 5 min after the start of perfusion were discarded. Following stabilization, hearts were analysed either with or without 50 nmol/L isoproterenol (Iso) added to the perfusate for the duration of the study.

### ECG Recording and Beating Rate Measurement

ECG was recorded on a single-lead Gould ACQ-7700 differential amplifier, digitized at 1 ms with DSI Ponemah software. Beating rate (BR) was calculated from the R-R intervals of the ECG using the P3S software. Baseline BR was determined for nontreated and Iso-treated (5 min. after stimulation) hearts. Negative chronotropic effects of carbachol (CCh) were examined by measuring BR changes following increasing concentrations of agonist (5 minute intervals). Animals that lost a normal ECG trace during recording were not included in BR analysis at subsequent doses. After addition of the highest CCh dose, the agonist was washed out and proper recovery of the ECG trace and BR was examined.

### Isolation and electrophysiologic recording from mouse sinoatrial node myocytes

The procedures for isolating single pacemaker myocytes from the sinoatrial node (SAN), as well from the mouse have been described previously<sup>4,6</sup> and were as follows. Mice were administered a 0.2 ml intraperitoneal injection of heparin (1000 IU/ml) to prevent blood clotting and given 5 minutes for it to be absorbed. Following this, mice were anesthetized with isoflurane and then killed by cervical dislocation. The heart was excised into Tyrode's solution (35°C) consisting of (in mmol/L) 140 NaCl, 5.4 KCl, 1.2 KH<sub>2</sub>PO<sub>4</sub>, 1.0 MgCl<sub>2</sub>, 1.8 CaCl<sub>2</sub>, 5.55 glucose, and 5 HEPES, with pH adjusted to 7.4 with NaOH. The sinoatrial node (SAN) region of the heart was isolated by separating the atria from the ventricles, cutting open the superior and inferior vanae cauae, and pinning the tissue so that the crista terminalis could be identified. The SAN area is located in the intercaval region adjacent to the crista terminalis. This SAN region was cut into strips, which were transferred and rinsed in a 'low Ca<sup>2+</sup>, Mg<sup>2+</sup> free' solution containing (in mmol/L) 140 NaCl, 5.4 KCl, 1.2 KH<sub>2</sub>PO<sub>4</sub>, 0.2 CaCl<sub>2</sub>, 50 taurine, 18.5 glucose, 5 HEPES and 1 mg/ml bovine serum albumin (BSA), with pH adjusted to 6.9 with NaOH. SAN tissue strips were digested in 5 ml of 'low Ca<sup>2+</sup>, Mg<sup>2+</sup> free' solution containing collagenase (type II, Worthington Biochemical Corporation), elastase (Worthington Biochemical Corporation) and protease (type XIV, Sigma Chemical Company) for 30 min. Then the tissue was transferred to 5 ml of modified KB solution containing (in mmol/L) 100 potassium glutamate, 10 potassium aspartate, 25 KCl, 10 KH<sub>2</sub>PO<sub>4</sub>, 2 MgSO<sub>4</sub>, 20 taurine, 5 creatine, 0.5 EGTA, 20 glucose, 5 HEPES, and 0.1% BSA, with pH adjusted to 7.2 with KOH. The tissue was mechanically agitated using a wide-bore pipette. This procedure yielded a sufficient number of SAN myocytes with cellular automaticity that was recovered after readapting the cells to a physiological concentration of Ca<sup>2+</sup>. SAN myocytes were identified by their small spindle shape and ability to beat spontaneously in the recording chamber when superfused with normal Tyrode's solution. The capacitance of single SAN myocytes was 20 – 35 pF.

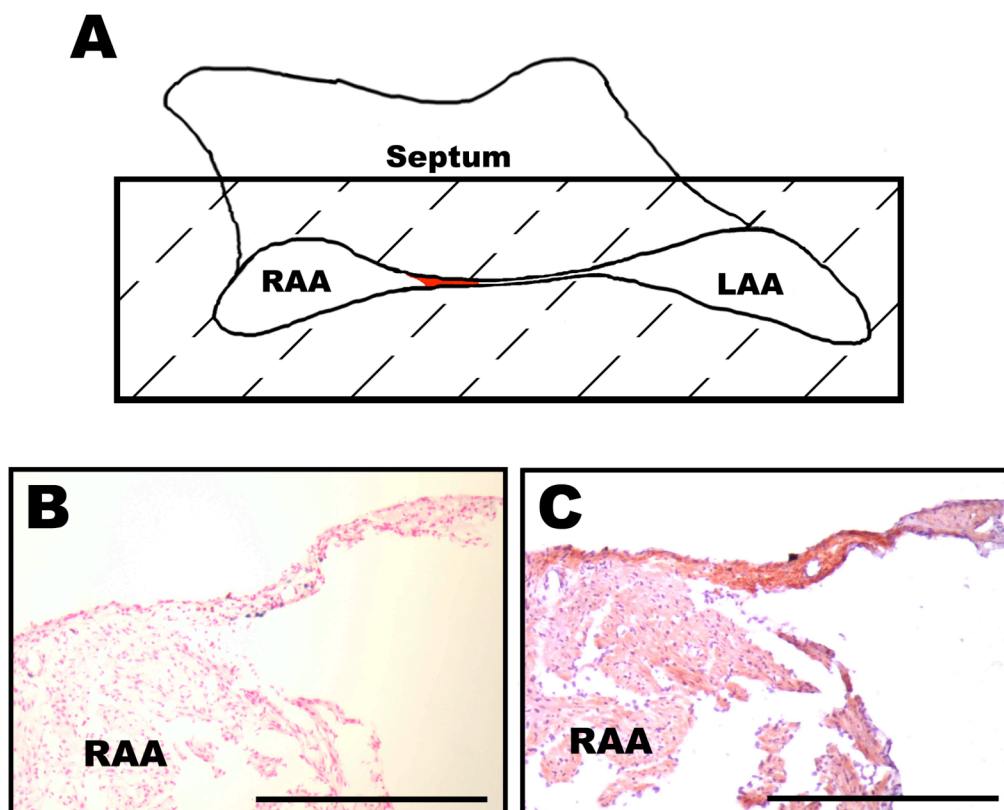
### Solutions and electrophysiological protocols

Spontaneous action potentials (APs) were recorded using the perforated patchclamp techniques on single SAN myocytes<sup>7, 8</sup>. Acetylcholine sensitive K<sup>+</sup> current (I<sub>K<sub>ACh</sub></sub>) was recorded by voltage clamping single SAN myocytes using the patch-clamp technique in the whole cell configuration<sup>8, 9</sup>. APs and membrane currents were recorded at room temperature (22-23 °C), which must be noted when comparing these data to the *in vivo* heart rate measurements. The effects of CCh (1 x 10<sup>-7</sup> mol/L) on spontaneous AP frequency were investigated. I<sub>K<sub>ACh</sub></sub> was investigated using a voltage ramp from +50 to -120 mV (holding potential was -75 mV) before and after the application of 1 x 10<sup>-5</sup> mol/L CCh. The CCh-sensitive difference currents were analyzed as described previously<sup>4</sup>.

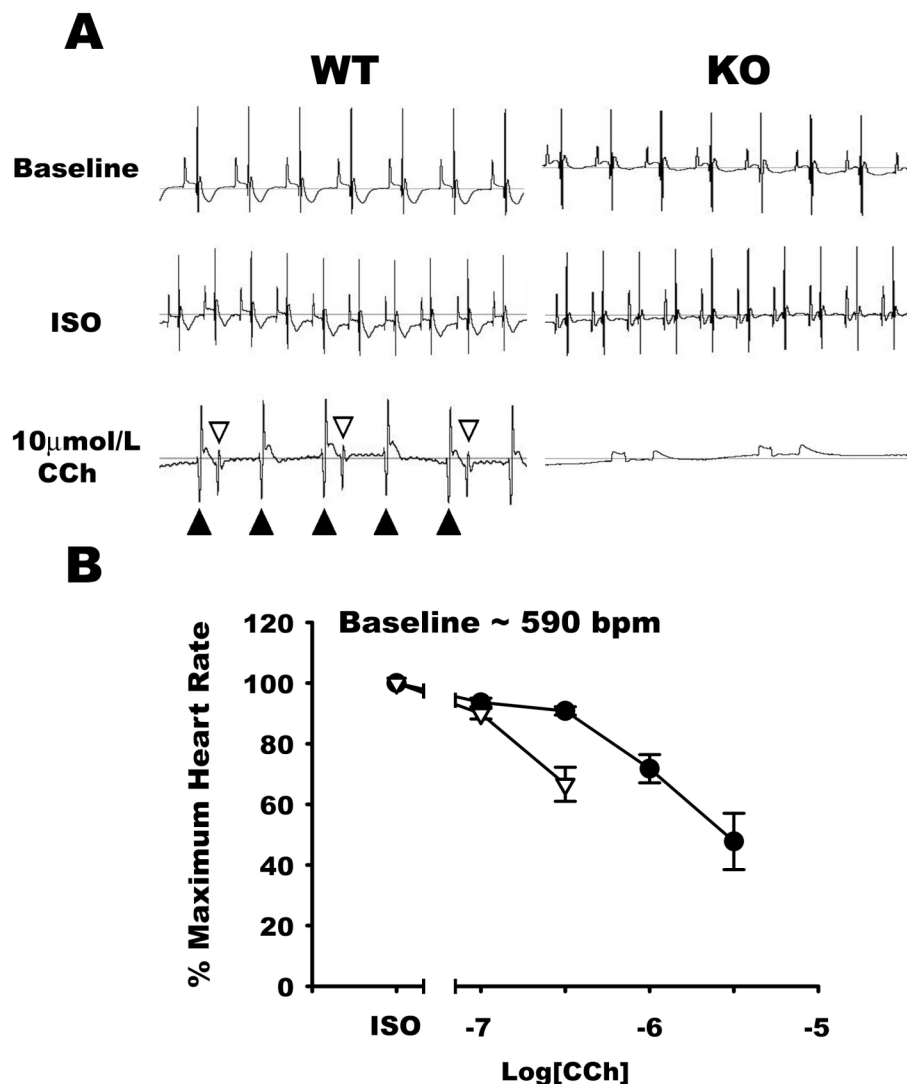
For recording both APs and  $I_{K_{ACh}}$ , the recording chamber was superfused with a normal Tyrode's solution (22 – 23°C) containing (in mmol/L) 140 NaCl, 5 KCl, 1 MgCl<sub>2</sub>, 1 CaCl<sub>2</sub>, 10 HEPES, and 5 glucose, with pH adjusted to 7.4 with NaOH. The pipette filling solution for  $I_f$  and  $I_{K_{ACh}}$  contained (in mmol/L) 135 KCl, 0.1 CaCl<sub>2</sub>, 1 MgCl<sub>2</sub>, 5 NaCl, 10 EGTA, 4 Mg-ATP, 6.6 Na-phosphocreatine, 0.3 Na-GTP and 10 HEPES, with pH adjusted to 7.2 with KOH. Amphotericin B (200 µg/ml) was added to this pipette solution to record APs with the perforated patch clamp technique.

Micropipettes were pulled from borosilicate glass (with filament, 1.5 mm OD, 0.75 mm ID, Sutter Instrument Company) using a Flaming/Brown pipette puller (model p-87, Sutter Instrument Company). The resistance of these pipettes was 5 – 8 MΩ when filled with recording solution. Micropipettes were positioned with a micromanipulator (Burleigh PCS-5000 system) mounted on the stage of an inverted microscope (Olympus IX51). Seal resistance was 2 – 15 GΩ. Rupturing the sarcolemma in the patch for voltage clamp experiments resulted in access resistances of 5 – 15 MΩ. Series resistance compensation averaged 80 – 85% using an Axopatch 200B amplifier (Molecular Devices). Data were digitized using a Digidata 1322A and pCLAMP 9 software (Molecular Devices) and stored on computer for *post hoc* analysis.

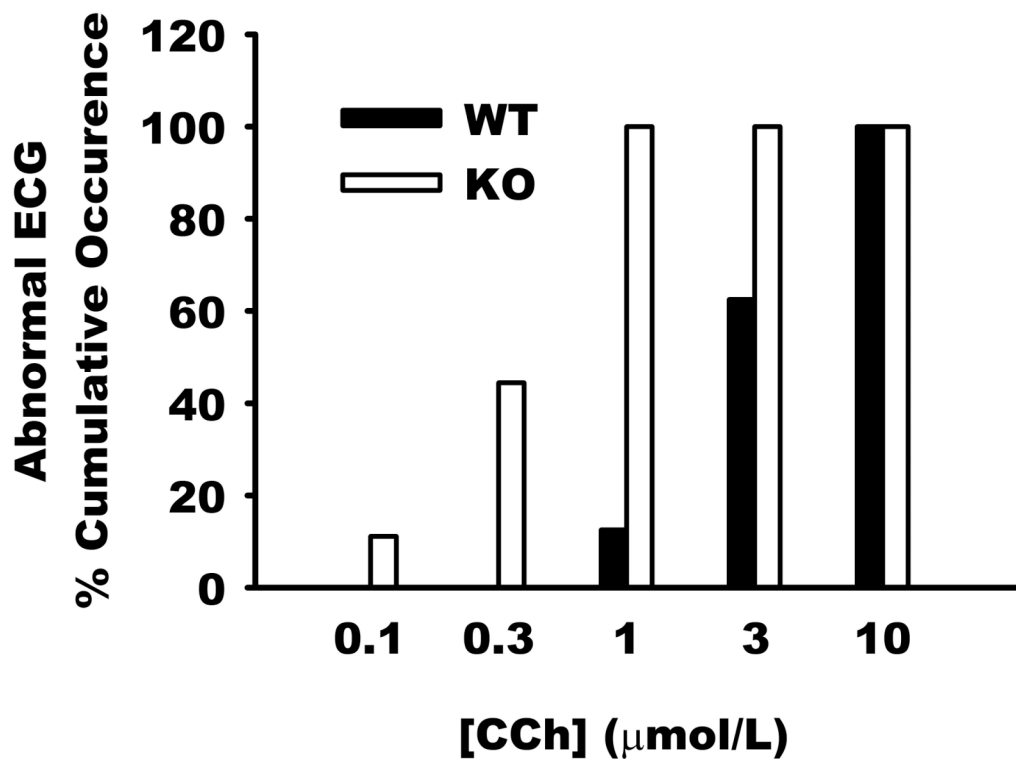
## RESULTS



**Supplemental Figure I.** Schematic of atrial preparation, showing cross section orientation relative to the SAN (red). Cross sections are shown as enlarged images of highlighted area in schematic. Left, *10x magnification* of LacZ stain with Nuclear fast red counterstain. Right, *10x magnification* of HCN4 stain with hematoxylin counter stain. LAA, left atrial appendage; RAA, right atrial appendage. *Scale bars* = 500 micrometers.



**Supplemental Figure II.** Increased negative chronotropy and loss of normal ECG trace in isolated RGS4-null hearts. A, Representative ECG traces of isolated RGS4-null (KO) and wild-type (WT) hearts at baseline and with  $5 \times 10^{-8}$  mol/L Iso. KO hearts show deterioration of the ECG at  $1 \times 10^{-5}$  mol/L CCh compared to WT hearts. By contrast  $1 \times 10^{-5}$  mol/L CCh typically produced atrioventricular dissociation in WT animals that is denoted by the different frequencies of the P wave (white arrow heads) and QRS complex (black arrow heads). Trace amplitudes are normalized for comparison. B,  $M_2R$ -mediated negative chronotropic responses and conduction defects are more pronounced in hearts isolated from *RGS4KO* compared to WT littermate control mice ( $n = 8$  hearts for WT and  $n = 9$  hearts for KO). Isolated hearts were cannulated and perfused in a retrograde fashion. Beating rate (BR) was determined from the R-R intervals of an ECG trace. The effect of increasing concentrations of the  $M_2R$  agonist CCh were examined in Iso ( $5 \times 10^{-8}$  mol/L)-stimulated hearts. Average BRs were expressed as a percentage of the Iso stimulated BR. Hearts that did not display a normal ECG following CCh treatment were scored as indeterminate and removed from BR analysis.



**Supplemental Figure III.** Cumulative occurrence of CCh-induced deterioration of normal ECG trace is increased in KO hearts. The quantification of indeterminable ECG traces in response to CCh shows that KO hearts experience deterioration of normal ECG (P-wave followed by QRS) at lower CCh concentrations than wild-type.

**Supplemental Table I. Summary of ECG response to CCh addition and washout.**

Genotype	# Hearts with AV Dissociation	# Hearts with loss of discernible ECG	# Hearts with full QRS recovery	# Hearts showing P-wave recovery
WT	8 / 8	0/8	7 / 8	8 / 8
KO	0 / 7	7/7	0 / 7	7 / 7

## Reference List

- (1) Kurrasch DM, Huang J, Wilkie TM, Repa JJ. Quantitative real-time polymerase chain reaction measurement of regulators of G-protein signaling mRNA levels in mouse tissues. *Methods Enzymol.* 2004;389:3-15.
- (2) Liu J, Dobrzynski H, Yanni J, Boyett MR, Lei M. Organisation of the mouse sinoatrial node: structure and expression of HCN channels. *Cardiovasc Res.* 2007;73:729-38.
- (3) Heximer SP, Knutsen RH, Sun X, Kaltenbronn KM, Rhee MH, Peng N, Oliveira-dos-Santos A, Penninger JM, Muslin AJ, Steinberg TH, Wyss JM, Mecham RP, Blumer KJ. Hypertension and prolonged vasoconstrictor signaling in RGS2-deficient mice. *J Clin Invest.* 2003;111:445-52.
- (4) Lomax AE, Rose RA, Giles WR. Electrophysiological evidence for a gradient of G protein-gated K<sup>+</sup> current in adult mouse atria. *Br J Pharmacol.* 2003;140:576-84.
- (5) Mangoni ME, Nargeot J. Properties of the hyperpolarization-activated current (I<sub>f</sub>) in isolated mouse sino-atrial cells. *Cardiovasc Res.* 2001 October;52:51-64.
- (6) Rose RA, Lomax AE, Kondo CS, Anand-Srivastava MB, Giles WR. Effects of C-type natriuretic peptide on ionic currents in mouse sinoatrial node: a role for the NPR-C receptor. *Am J Physiol Heart Circ Physiol.* 2004;286:H1970-H1977.
- (7) Rae J, Cooper K, Gates P, Watsky M. Low access resistance perforated patch recordings using amphotericin B. *J Neurosci Methods.* 1991;37:15-26.
- (8) Rose RA, Kabir MG, Backx PH. Altered heart rate and sinoatrial node function in mice lacking the cAMP regulator phosphoinositide 3-kinase-gamma. *Circ Res.* 2007;101:1274-82.
- (9) Hamill OP, Marty A, Neher E, Sakmann B, Sigworth FJ. Improved patch-clamp techniques for high-resolution current recording from cells and cell-free membrane patches. *Pflugers Arch.* 1981;391:85-100.